Chapter 2

Direct Numerical Simulation of Hydrate Dissociation in Homogeneous Porous Media by Applying CFD Method: One Example of CO_2 Hydrate

Wu-Yang Sean

Additional information is available at the end of the chapter

http://dx.doi.org/10.5772/intechopen.74874

Abstract

Computational fluid method (CFD) is popular in either large-scale or meso-scale simulations. One example is to establish a new pore-scale (m~μm) model of laboratory-scale sediment samples for estimating the dissociation rate of synthesized CO_2 hydrate (CO_2H) reported by Jeong. It is assumed that CO_2H formed homogeneously in spherical pellets. In the bulk flow, concentration and temperature of liquid CO_2 in water flow was analyzed by CFD method under high-pressure state. Finite volume method (FVM) were applied in a face-centered packing in unstructured mesh. At the surface of hydrate, a dissociation model has been employed. Surface mass and heat transfer between hydrate and water are both visualized. The initial temperature 253.15K of CO_2H pellets dissociated due to ambient warm water flow of 276.15 and 282.15K and fugacity variation, ex. 2.01 and 1.23 MPa. Three tentative cases with porosity 74, 66, and 49% are individually simulated in this study. In the calculation, periodic conditions are imposed at each surface of packing. Numerical results of this work show good agreement with Nihous' model. Kinetic modeling by using 3D unstructured mesh and CFD scheme seems a simple tool, and could be easily extended to determine complex phenomena coupled with momentum, mass and heat transfer in the sediment samples.

Keywords: heat and mass transfer, finite volume method (FVM), computational fluid dynamics (CFD), pore-scale flow

1. Introduction

Computational fluid method (CFD) is popular in either large-scale or meso-scale simulations. One example is to establish a new pore-scale (m~μm) model of laboratory-scale sediment

samples for estimating the dissociation rate of synthesized CO_2 hydrate (CO_2H) reported by [1]. To decrease the CO_2 concentration in the air, carbon dioxide capture and storage (CCS) is regarded to be an effective way. One concept of CCS is to store CO_2 in gas hydrate in sub-seabed geological formation, as was illustrated by [6]. Besides, many studies about the formation and dissociation of CO_2 hydrate (CO_2H) while stored in the deep ocean or geologic sediment have been introduced. In particular, flow and transport in sediment is multidisciplinary science including the recovery of oil, groundwater hydrology and CO_2 sequestration. It reported the measurements of the dissociation rate of well-characterized, laboratory-synthesized carbon dioxide hydrates in an open-ocean seafloor [5]. The pore effect in the phase equilibrium mainly due to the water activity change was discussed in [7]. The reactive transport at the pore-scale to estimate realistic reaction rates in natural sediments was discussed in [3]. This result can be used to inform continuum scale models and analyze the processes that lead to rate discrepancies in field applications. Pore-scale model is applied to examine engineered fluids [4]. Unstructured mesh is well suited to pore-scale modeling because of adaptive sizing of target unit with high mesh resolution and the ability to handle complicated geometries [17, 18]. Particularly, it can easily be coupled with computational fluid dynamics (CFD) methods, such as finite volume method (FVM) or finite element method (FEM). Unstructured tetrahedral mesh used to define the pore structure is discussed in [19]. Another case includes a numerical simulation of laminar flow based on FVM with unstructured meshes was used to solve the incompressible, steady Navier-Stokes equations through a cluster of metal idealized pores by [20].

The objective of this work is to develop a new pore-scale model for estimating the dissociation rate of CO_2H in homogeneous porous media. To cooperate with molecular simulation and field-scale simulators, we aim at establishing pore-scale modeling to analyze the simultaneous kinetic process of CO_2H dissociation due to non-equilibrium states. Major assumptions in this study are listed as below:

1. Only dissociation occurred at the surface, no any formation occurred immediately with dissociation.
2. CO_2 dissociated at the surface is assumed to be dissolved into liquid water totally without considering the gas nucleated.
3. The surface structure does not collapse with the dissociation of CO_2H at the surface of pellets.
4. Homogeneous face-centered packing of multi-CO_2H pellets.
5. Single phase flow coupled with mass, heat, and momentum transfers.

2. Dissociation modeling at the surface

In this study, the dissociation flux (F_1) is assumed to be proportional to the driving force, the free energy difference ($\Delta\mu$) introduced by [6], presented as

$$F_1 = k_{\mathrm{bl}} \mathrm{RT} \ln\left(\frac{C_{Hsol}}{C_I}\right) \tag{1}$$

http://dx.doi.org/10.5772/intechopen.74874

where k_{bl} is the rate constant $\left[\text{mol}^2\ \text{J}^{-1}\ \text{s}^{-1}\text{m}^{-2}\right]$ of dissociation. According to [21], k_{bl} is listed as below:

$$k_{bl} = \exp\left(-\frac{11,729}{T} + 26.398\right) \tag{2}$$

where C_{Hsol} is the mole fraction of CO_2 in the aqueous solution at equilibrium state with hydrate, and C_I means surface concentration in the ambient aqueous solution at the surface of the hydrate C_I.

3. Basic transport equations

Flow in the porous media around CO_2H is governed by the continuity and the Navier-Stoke's equations. The advection-diffusion equations of non-conservative type for mass concentration C and temperature T are also considered.

$$\nabla \cdot \mathbf{u} = 0 \tag{3}$$

$$\frac{\partial \mathbf{u}}{\partial t} + \nabla \cdot (\mathbf{uu}) = -\nabla P + \frac{1}{\text{Re}} \nabla \cdot \left[\nabla \mathbf{u} + (\nabla \mathbf{u})^T\right] + \frac{\rho_w}{\text{Fn}^2} g \tag{4}$$

No.	Function	Definition
1	$D = 7.4 \times 10^{-12} \frac{(\varphi M_B)^{1/2} T}{\eta_L V_A^{0.6}}$	D: diffusion coefficient of CO_2 in water φ(=2.6): association parameter for the solvent water $M_B\left(= 18\ \text{gmol}^{-1}\right)$: molecular weight of water $V_A\left(= 3.4 \times 10^{-5}\ \text{m}^3\text{mol}^{-1}\right)$: molar volume of CO_2 η_L[mPa·s]: viscosity of water
2	$\nu_L = \left(8.8286 \times 10^{-10}\right)T^2 - \left(5.3886 \times 10^{-7}\right)T + 8.314 \times 10^{-5}$	$\nu_L\left[\text{ms}^{-2}\right]$: kinematic viscosity
3	$\lambda_L = 487.85\ln(T) - 2173.8$	$\lambda_L\left[\text{WKm}^{-1}\right]$: heat conductivity of water
4	$\alpha_L = \frac{\lambda_L}{\rho_W C_p}$	$\alpha_L\left[\text{ms}^{-2}\right]$: the thermal diffusivity of aqueous phase $\rho_W\left(= 997.1 \frac{\text{kg}}{\text{m}^3}\right)$: density of water $C_p\left(= 4,180 \frac{\text{J}}{\text{kg}} \cdot \text{K}\right)$: isobaric specific heat, quoted from "Chemical Engineering Handbook", Japan (1985)
5	$P_{eq} = \exp\left(\alpha + \frac{\beta}{T}\right) \times 10^3$	α=44.580 and β = − 10246.28
6	$C_{Hsol} = a \cdot \exp\left(b \cdot P \times 10^{-6} + 1.321 \times 10^{-4} T - 2.292 \times 10^{-2}\right) \cdot 1.8 \times 10^{-5}$	$C_{Hsol}\left[\text{mole} \cdot \text{m}^{-3}\right]$: solubility of hydrate (275.15 K < T < 281.15 K) $a = 0.0016(T - 273.15)^{0.9211}$ $b = -0.0199\log(T - 273.15) + 0.0942$ by Aya et al. [10], Yang et al. [11], and Servio and Englezos [12]

Table 1. Parameters used in this study.

$$\frac{\partial C}{\partial t} + \mathbf{u} \cdot \nabla C = \frac{1}{\mathrm{ReSc}} \nabla^2 C \tag{5}$$

$$\frac{\partial T}{\partial t} + \mathbf{u} \cdot \nabla T = \frac{1}{\mathrm{RePr}} \nabla^2 T \tag{6}$$

where the viscosity, diffusivity, and thermal conductivity of pure water are included in dimensionless parameters such as the Reynolds number, the Schmit number, and the Prandtl number, which are interpolated as functions of temperature and are updated at every computational time step as summarized in **Table 1**. U and d (=0.001 m) are the velocity of inflow and diameter of hydrate pellet.

4. Mass transfer

To rewrite Eq. (1), the flux at the surface of the hydrate can be discretized as

$$k_{bl} RT \ln\left(\frac{C_{Hsol}}{C_I}\right) = D\nabla C = D\frac{C_I - C'}{h_I} \tag{7}$$

where C_I is the varying surface concentration calculated locally at each surface cell, C' is the centroid concentration, and h_I is the thickness of centroid surface cell, as shown in **Figure 1**.

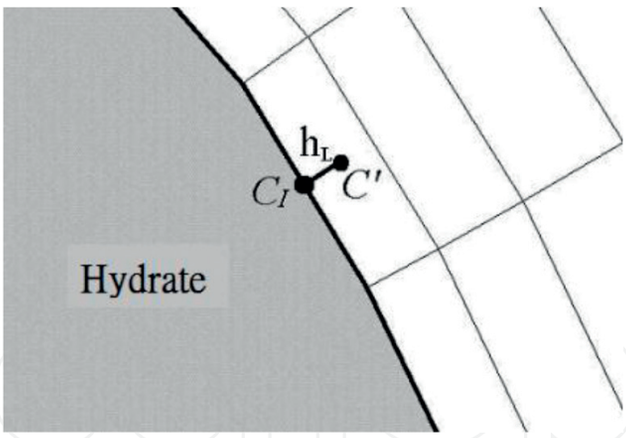

Figure 1. Schematic image of discretized surface concentration.

5. Heat transfer

The equation of energy balance at the surface of CO_2H is given by

$$\dot{Q}_H + \lambda_H \nabla T_H = \lambda_L \nabla T_L \tag{8}$$

http://dx.doi.org/10.5772/intechopen.74874

where $\dot{Q}_H$ (= $H_L F_1$, where H_L is the latent heat of hydrate dissociation) is the dissociation heat transferred to the CO_2H, λ_H is the thermal conductivity of hydrate. Dissociation heat per mole of hydrate, H_L, is interpolated from [2] as

$$H_L = 207,917 - 530.97 \times T_I \tag{9}$$

where T_I is the surface temperature. Then, we have

$$T_I = \frac{\lambda_L h_H T_L + \lambda_H h_L T_H - 207,917 \cdot F_{cal} h_L h_H}{\lambda_L h_H + \lambda_H h_L - 530.97 \cdot F_{cal} h_L h_H} \tag{10}$$

where T_L and T_H are the temperatures defined at the centroids cell in the aqueous phase and solid hydrate, respectively; h_L and h_H are half widths of centroid in the aqueous phase and solid hydrate, respectively. Besides, the temperature in the pellet is calculated by using the heat conductivity equation.

$$\frac{\partial T}{\partial t} = \alpha_H \frac{\partial^2 T}{\partial x^2} \tag{11}$$

where $\alpha_H = \frac{\lambda_H}{\rho_H C_p'}$ is the thermal diffusivity of CO_2H. These relative properties of CO_2H are quoted from [9], the thermal diffusivity of aqueous phase (α_H) of $1.38 \times 10^{-7} ms^{-2}$, the heat capacity of hydrate (C_p') of $2080.0\ JK^{-1}kg^{-1}$, and the thermal conductivity (λ_H) of $0.324\ WK^{-1}m^{-1}$. The density of CO_2H (ρ_H) is given as $1116.8\ kgm^{-3}$.

6. Computational conditions

Two types of cells, tetrahedrons and triangular prisms, are applied in the present unstructured grid system, as introduced in **Figure 2**. In detailed, the surface of hydrate uses prism. Both the flow field and inside the pellet are tetrahedral meshes. Upward is the inflow where initially the uniform velocity profile is adopted. Prism mesh and no-slip condition are imposed at the surface of the pellet. To analyze more detailed mass and heat transfer simulatneously, one cell-layer of the prisms that attached to the CO_2H surface is divided into at least five very thin layers as referred in [8] for high Prandtl or Schmidt number. The basic parameters of computation are denoted in **Table 1**. The initial values of dimensionless parameters are listed in **Table 2** at the temperatures from 276.15 to 283.15 K. Reynolds number, Schmidt number, and Prandtl number function of the temperature or pressure are listed in **Table 2**. The minimum grid size of this computational model is listed in **Table 3**. Lm, Lc, and LT are the applied mesh thicknesses. δm, δc, and δT are the thickness of momentum, concentration, and thermal boundary layers, respectively. The relationship between δm, δc, and δT quoted from the theory of flat plate boundary layer is listed below:

$$\delta_m = \frac{5.48}{\sqrt{\mathrm{Re}}}\frac{d}{2} \tag{12}$$

$$\delta_c = \frac{\delta_m}{1.026 \cdot Sc^{1/3}} \tag{13}$$

$$\delta_T = \frac{\delta_c}{\mathrm{Pr}^{1/3}} \tag{14}$$

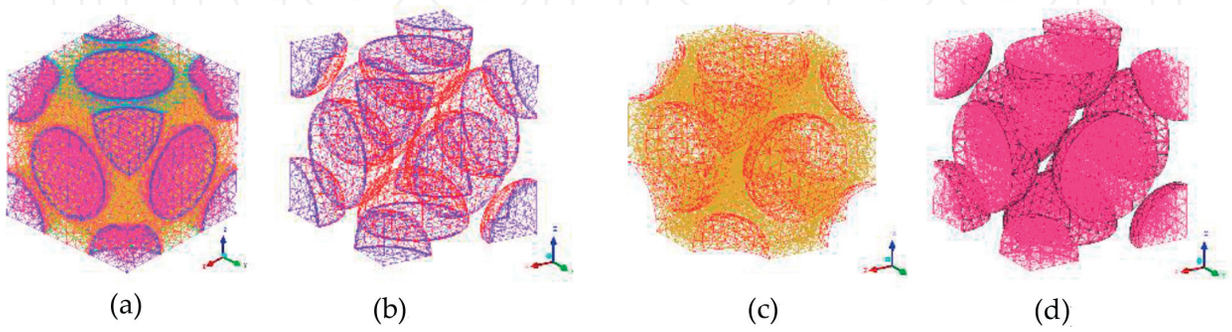

Figure 2. Description of mesh in unstructured grid system of 67,104 cells. (a) Overview, (b) surface of CO_2H, (c) water, and (d) pellets of CO_2H.

Case	Reynold number	Prandtl number	Froude number	Schmidt number	Porous ratio	Temperature of water (K)	Fugacity of equilibrium (MPa)	Fugacity (MPa)
1	50	10	0.023	755	74%	282.15	3.89	3
2		12		880		276.15	1.77	1
3		10		755	66%	282.15	3.89	3
4		12		880		276.15	1.77	1
5		10		755	49%	282.15	3.89	3
6		12		880		276.15	1.77	1
7	100	10	0.046	755		282.15	3.89	3
8	135		0.062					

Table 2. Calculation conditions of this work.

Cell number (porosity)	Sc*	δ_m*	$\delta_{c\&T}$*	L_m	VTL number	$L_{c\&T}$
53,440 (49%)	755	2.358E-04	2.252E-05	1.0E-05	5	2.0E-06
67,104 (66%)	755	2.345E-03	2.252E-04	6.0E-05	5	1.2E-05
77,432 (74%)	755	2.594E-03	2.276E-04	6.0E-05	5	1.2E-05

*Values are quoted from "Chemical Engineering Handbook", Japan (1985)

Table 3. The thicknesses of boundary layers, δ_m and $\delta_{c\&T}$, and grid sizes, L_m and $L_{c\&T}$ (unit: meter).

http://dx.doi.org/10.5772/intechopen.74874

To follow [22] of Eq. (14), the boundary layer's thickness for temperature, δ_T is assumed as the same size as that for mass concentration, δ_c. For the initial temperature of the CO_2H pellet, T_{ini} is assumed as a constant value of 253.15 K.

7. Verification

The in-house code originally developed by [7] has been applied to determine the intrinsic dissociation rate of methane hydrate. The numerical results verified by experimental results are successfully used in calculating one pellet of hydrate in a slow flow rate of high pressure without considering the collapse of hydrate and the nucleation of bubbles referring to [6, 20] as well.

8. Results of case study

In this study, cases with porosity of 74, 66, and 49 are individually discretized as face-centered unstructured packing of hydrate in sediment. CO_2H pellets with initial temperature of 253.15 K dissociate due to the variation of driving force, ex. 0.89 and 0.77 MPa, under thermal stimulation of ambient warm water, ex. 282.15 and 276.15 K. Comparative small driving forces selected here is due to the assumption of no surface's collapse. Computational conditions are listed in **Table 2**. Result of flux at the surface is the converge value as shown in **Figure 3**. In **Figure 4(a)–(c)** at time 0.16(s) show velocity vector of case 1 in three specific sections. In **Figure 5**, the distributions of concentration at 0.16 s are presented. Slight CO_2 discharges at the surface. Relative temperature distributions are indicated in **Figure 6**. As time increases, the dissociation heat of CO_2 hydrate results in water temperature drop significantly as shown in

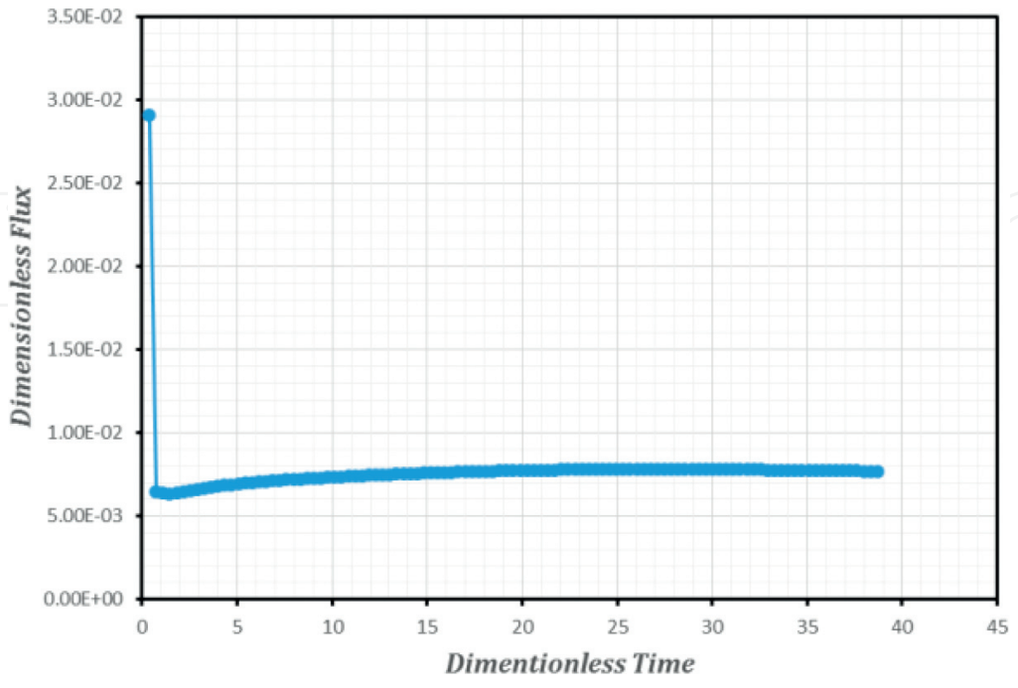

Figure 3. Converge value of case 1.

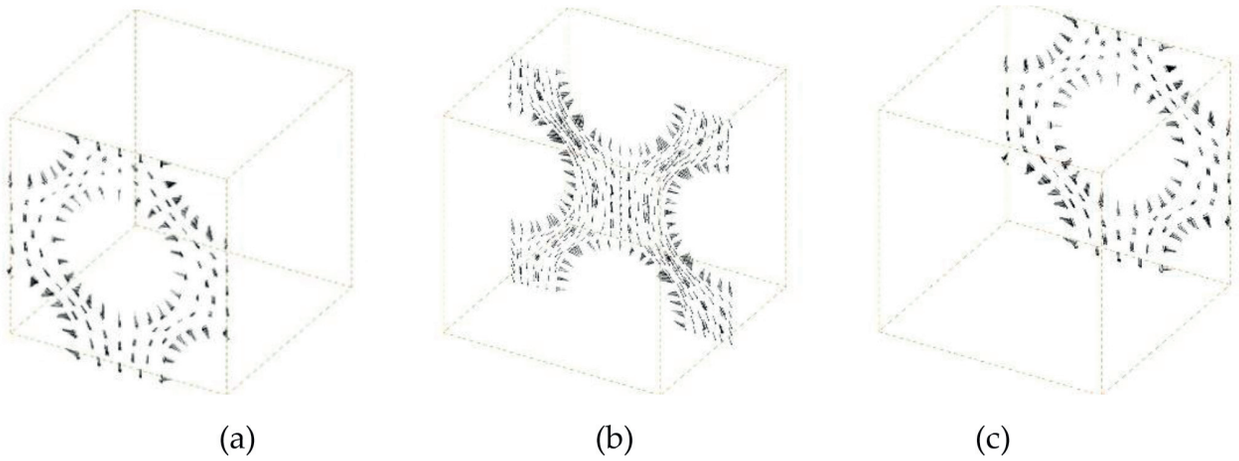

Figure 4. Velocity vector in the vicinity of pellets (case 1: T = 282.15 K, T_{ini} = 253.15 K, Re = 50, Sc = 755, Pr = 10, VTL = 5, and time = 0.16 s). (a) Front section, (b) Center section and (c) Back section.

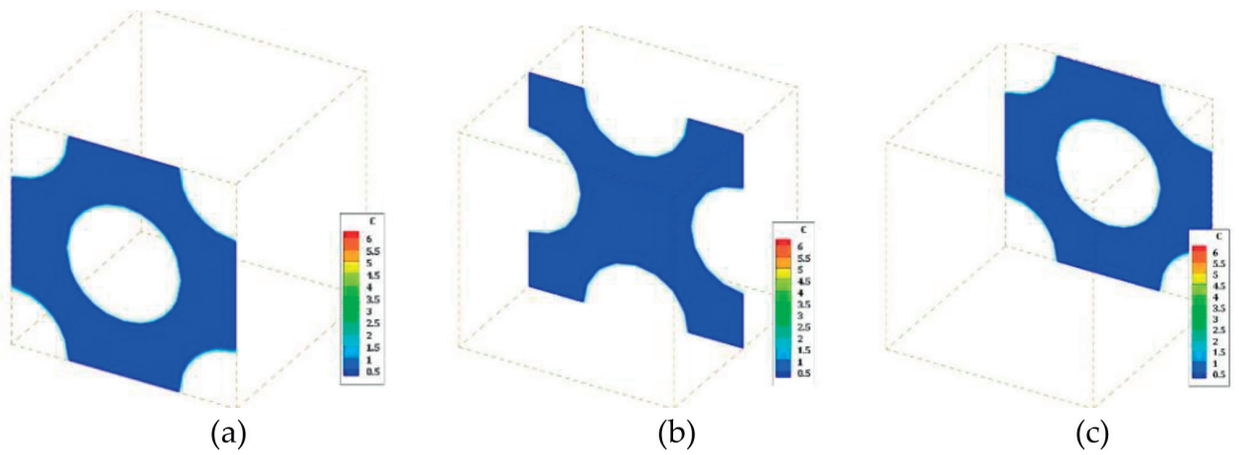

Figure 5. Concentration profile in three specific sections of cubic unit (case 1: time = 0.16 s, unit: mole/m^2 s). (a) Front section, (b) Center section and (c) Back section.

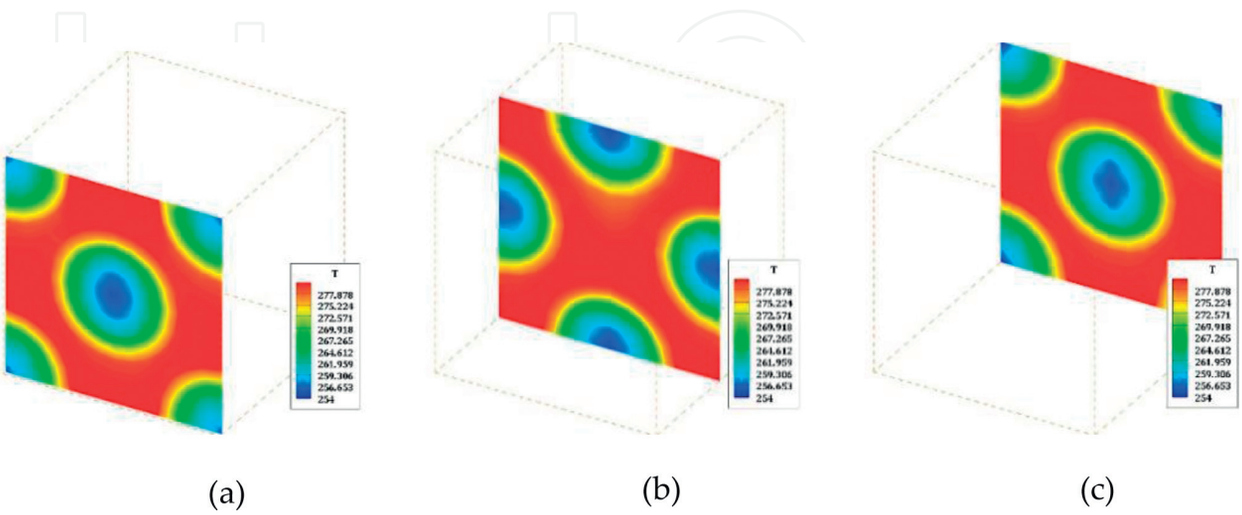

Figure 6. Temperature profile in three specific sections of cubic unit (case 1, time = 0.16 s, unit: K). (a) Front section, (b) Center section and (c) Back section.

http://dx.doi.org/10.5772/intechopen.74874

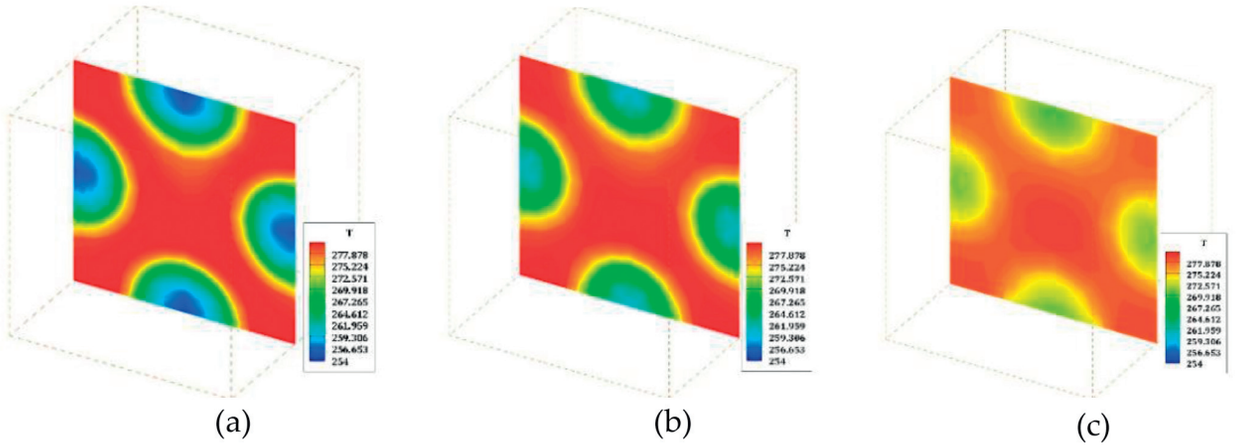

Figure 7. Temperature versus time in center section of cubic unit (case 1, time = 0.16 s, 0.27 s, and 0.54 s, unit: K). (a) Front section, (b) Center section and (c) Back section.

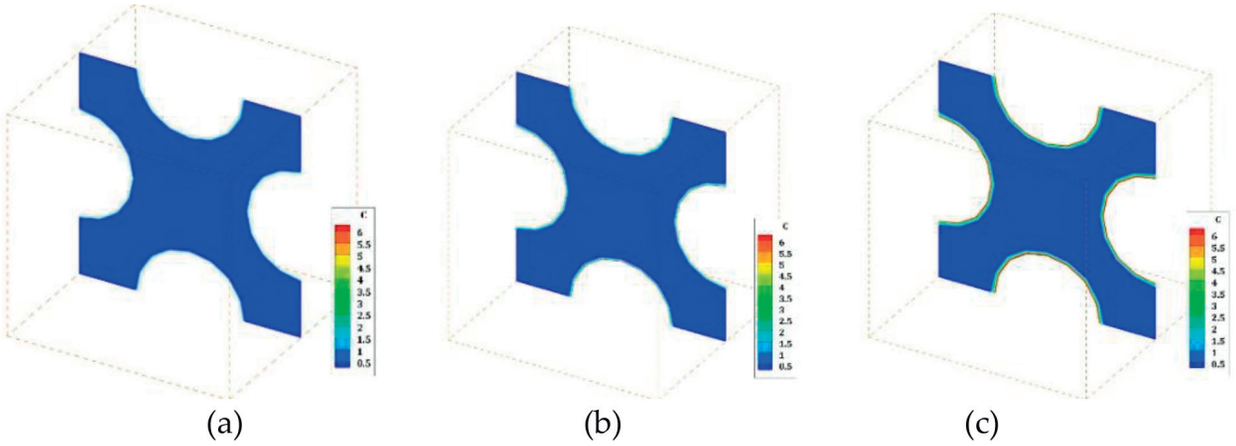

Figure 8. Concentration versus time in center section of cubic unit (case 1, time = 0.16 s, 0.27 s, and 0.54 s, unit: mole/m^2 s). (a) Front section, (b) Center section and (c) Back section.

Figure 7(a)–(c). Relative concentration distribution in center section is shown in **Figure 8**. The heat of water conducts to the solid-side pellet rapidly in few seconds, and slow mass transfer at the surface dominates the dissociation rate rather than fast heat transfer at the surface.

9. Discussion

To follow the modeling illustrated in [14]:

$$F_3 = k_D\left(f_{eq} - f_g\right) = k_{D0}\exp\left(-\frac{\Delta E}{RT}\right)\left(f_{eq} - f_g\right) \tag{15}$$

where $k_{D0}\left[\text{mol Pa}^{-1}\text{s}^{-1}\text{m}^{-2}\right]$ is the rate constant, $f_g(\text{Pa})$ is the fugacity of gaseous CO_2, and f_{eq} is the fugacity of the quadruple equilibrium. They obtained k_{D0} and ΔE for CO_2H as 1.83×10^8 mol Pa^{-1}s^{-1}m^{-2} and 102.88 kJ mol^{-1}, respectively, at temperature and pressure

ranging from 274.15 to 281.15 K and from 1.4 to 3.3 MPa. However, new modified value of ΔE, if considered the real case in the ocean quoted from [16], is 96.49 kJ mol^{-1}. The order of Reynolds number based on the size of a particle, about 16 μm, is calculated as 50. Clarke et al. [28] determined the dissociation rate of CO2H by measuring the nucleated methane gas in V-L state [14]. The comparison of three models is listed in **Table 4**. The results of dissociation flux are summarized in **Figure 9**. Higher water temperature induces higher dissociation flux at the surface of hydrate. Data correlated by [14] show much lower level than both Nihous' model and new model. The numerical results in this work marked as new model in **Figure 9** show consistent result compared with Nihous' model. The dissociation flux in various flow rates in cases 5, 7, and 8 are listed in **Figure 10**. Here, it is noted that porosity is not considered in both Clarke's and Nihous' models, and these two models are only function of temperature and fugacity as presented in Eq. (15). The trend of flux becomes saturated in the figure due to the surface dissociation flux that becomes slow due to the fast mass transfer in bulk flow at Reynolds number over 100.

Item	Modeling	Intrinsic rate of dissociation	Ref.
Clarke's Model	Eq. (15)	K_{D0} = 1.83 * 10^8mole/Pa s m; ΔE = 102.89 kJ/mole	[14]
Nihous' Model	Eq. (15)	K_{D0} = 1.83 * 10^8mole/Pa s m; ΔE = 96.49 kJ/mole	[16]
New Model	Eq. (1)	K_{bl} = exp(−11,729/T + 26,398)	[21]

Table 4. The comparison of three models.

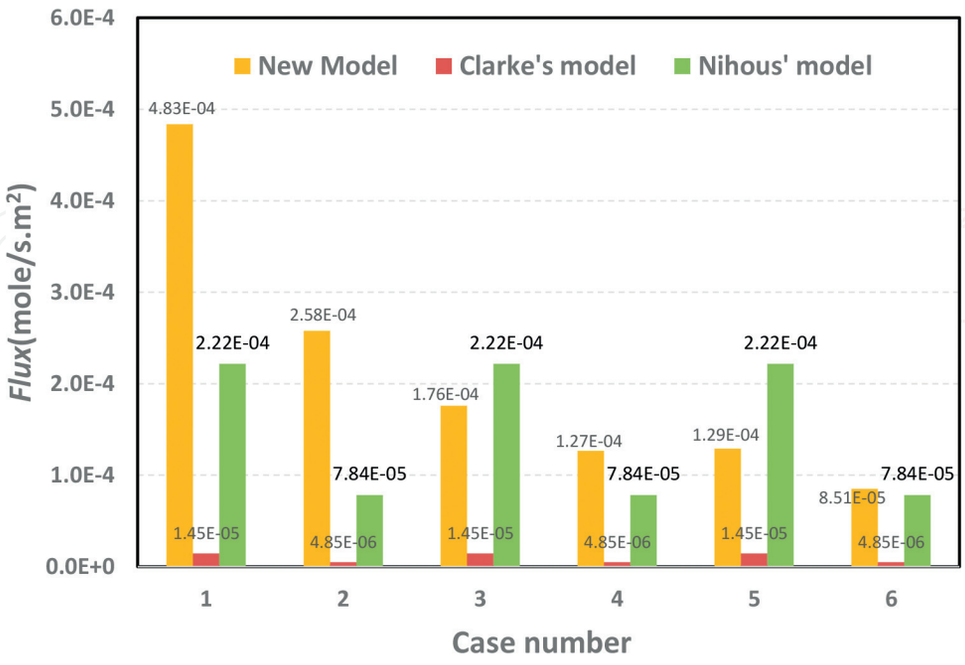

Figure 9. Results of simulation compared to existing two models.

http://dx.doi.org/10.5772/intechopen.74874

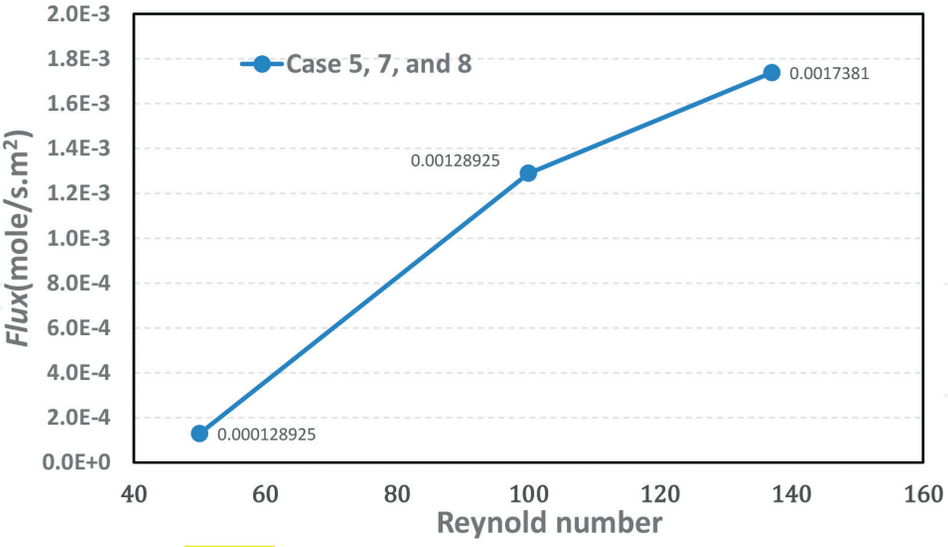

Figure 10. Results of flux in cases 5, 7, and 8.

10. Conclusions

The objective of this work is to establish a new pore-scale model for estimating the dissociation rate of CO_2H in laboratory-scale sediment samples. It is assumed that CO_2H formed homogeneously in spherical pellets. In the bulk flow, concentration and temperature of liquid CO_2 in water flow was analyzed by computational fluid dynamics (CFD) method without considering gas nucleation under high-pressure state. In this work, finite volume method (FVM) was applied in a face-centered regular packing in unstructured mesh. At the surface of hydrate, a dissociation model has been employed. Surface mass and heat transfer between hydrate and water are both visualized. The initial temperature 253.15 K of CO_2H pellets dissociated due to ambient warm water flow of 276.15 and 282.15 K and fugacity variation, ex. 2.01 and 1.23 MPa. Three tentative cases with porosity 74, 66, and 49% are individually simulated in this study. In the calculation, periodic conditions are imposed at each surface of packing. Additionally, the flux at CO_2H's surfaces is compared to Clarke and Bishnoi [13] and Nihous and Masutani [15] 's correlations at Reynolds number of 50. Numerical results of this work show good agreement with Nihous' model. Kinetic modeling by using 3D unstructured mesh of regular cubic unit and CFD scheme seems to be a simple tool to estimate the dissociation rate of CO_2H in laboratory-scale experiments, and could be easily extended to determine complex phenomena coupled with momentum, mass, and heat transfer in the sediment samples.

Acknowledgements

This work was supported by DOIT, Ministry of Science and Technology under contract No. MOST 106-3113-M-002-006. The authors also wish to acknowledge Professor Toru SATO for the valuable advices and guidance.

Nomenclature

C	volumetric molar concentration of CO_2 in the ambient water $\left[\text{mol m}^{-3}\right]$
C_H	volumetric molar concentration of CO_2 in the aqueous solution equilibrated with the stable hydrate phase $\left[\text{mol m}^{-3}\right]$
C'	volumetric molar concentration of CO_2 in water at the centroid of a cell attaching to the hydrate surface $\left[\text{mol m}^{-3}\right]$
C_I	volumetric molar concentration of CO_2 in the ambient aqueous solution at the surface of the hydrate ball $\left[\text{mol m}^{-3}\right]$
C_X	average molar volumetric concentration of CO_2 in the ambient water flow for a given cross section of water flow $\left[\text{mol m}^{-3}\right]$
d	diameter of the CO_2 hydrate ball [m]
D	diffusion coefficient of CO_2 in water $\left[\text{m s}^{-2}\right]$
E	activation energy $\left[\text{J mol}^{-1}\right]$
F	dissociation rate flux $\left[\text{mol s}^{-1}\ \text{m}^{-2}\right]$
f_{eq}	fugacity of the quadruple equilibrium [Pa].
f_g	fugacity of gaseous CO_2 [Pa]
G	molar Gibbs free energy $\left[\text{J mol}^{-1}\right]$
H_L	latent heat of hydrate dissociation $\left[\text{J mol}^{-1}\right]$
h_L	length of the water layer attached to the hydrate surface [m]
k_{D0}	intrinsic dissociate rate constant based on Clarke-Bishnoi model $\left[\text{mol Pa}^{-1}\text{s}^{-1}\text{m}^{-2}\right]$
k_{bl}	dissociation rate constant based on new model $\left[\text{mol}^2\ \text{J}^{-1}\ \text{s}^{-1}\text{m}^{-2}\right]$
L	thickness of computational cell [m]
M_B	molecular weight of water $\left[\text{g mol}^{-1}\right]$
P	thermodynamic pressure [Pa]
P_{eq}	quadruple equilibrium pressure for CO_2 hydrate as a function of T [Pa]
Q	volumetric flow rate of the ambient water $\left[\text{m}^3\text{s}^{-1}\right]$

http://dx.doi.org/10.5772/intechopen.74874

$\dot{Q}_H$	the rate at which the latent heat is transferred to the CO_2 hydrate by dissociation $\left[\mathrm{Jm^{-2}s^{-1}}\right]$
R	gas constant, 8.314 $\left[\mathrm{J\ K^{-1}\ mol^{-1}}\right]$
T	absolute temperature [K]
T_L	temperature at the centroids of a cell in the solid hydrate [K]
T_H	temperature at the centroids of a cell in the aqueous phase [K]
$\boldsymbol{u}$	velocity vectors [m/s]
x	mole fraction of CO_2 [-]
x_{eq}	solubility of CO_2 in the aqueous solution in equilibrium with the stable hydrate phase [-]
x_I	mole fraction of CO_2 in the aqueous phase at the surface of the hydrate ball [-]
α_L	thermal diffusivity in the aqueous phase $\left[\mathrm{m\ s^{-2}}\right]$
α_H	thermal diffusivity in the hydrate ball $\left[\mathrm{m\ s^{-2}}\right]$
Δr	thickness of the computational cell [m]
δ	thickness of the boundary layer [m]
$\Delta\mu$	chemical potential difference $\left[\mathrm{J\ mol^{-1}}\right]$
ρ_w	density of the ambient water $\left[\mathrm{kg\ m^{-3}}\right]$
φ	the association parameter for the solvent water
η_L	the viscosity of water [mPa s]
V_A	the molar volume of CO_2 $\left[\mathrm{m^3mol^{-1}}\right]$
ν_L	kinematic viscosity of water $\left[\mathrm{ms^{-2}}\right]$
λ_L	heat conductivity of water $\left[\mathrm{W\ K^{-1}\ m^{-1}}\right]$
λ_H and λ_L	the heat conductivities in the hydrate and water $\left[\mathrm{WK^{-1}m^{-1}}\right]$

Author details

Wu-Yang Sean

Address all correspondence to: wuyangsean@gmail.com

Department of Environmental Engineering, Chung Yuan Christian University, Taiwan

References

[1] Jeong S-M, Hsieh L-HC, Huang C-Y, Sean W-Y. Direct numerical simulation of CO_2 hydrate dissociation in pore-scale flow by applying CFD method. International Journal of Heat and Mass Transfer. 2017;**107**:300-306

[2] Andersson V, Kvaerner A, Haines M. Gas hydrates for deep ocean storage of CO_2—novel technology for utilising hydrates for transport of CO_2. In: Wilson M, Morris T, Gale J, Thambimuthu K, editors. Greenhouse Gas Control Technologies, Volume II. New York: Elsevier; 2005. pp. 1487-1492

[3] Molins S, Trebotich D, Steefel CI, Shen C. An investigation of the effect of pore scale flow on average geochemical reaction rates using direct numerical simulation. Water Resources Research. 2012;**48**:7453-7460. DOI: 10.1029/2011WR011404

[4] Davison SM, Yoon H, Martinez MJ. Pore scale analysis of the impact of mixing-induced reaction dependent viscosity variations. US Department of Energy Publications. Paper 110. 2012. http://digitalcommons.unl.edu/usdoepub/110

[5] Gregor R, Stephen HK, William BD, Laura AS, Edward TP, John P, Peter GB. Dissolution rates of pure methane hydrate and carbon-dioxide hydrate in undersaturated seawater at 1000-m depth. Geochimica et Cosmochimica Acta. 2004;**68**(2):285-292

[6] Inui M, Sato T. Economical feasibility study on CO_2 sequestration in the form of hydrate under seafloor. Proceedings of 26th International Conference on Offshore Mechanical and Arctic Engineering. 2006;OMAE06-92306:1-10

[7] Uchida T, Ebinuma T, Takeya S, Nagao J, Narita H. Effects of pore sizes on dissociation temperatures and pressures of methane, carbon dioxide, and propane hydrates in porous media. The Journal of Physical Chemistry. B. 2002;**106**:820-826

[8] Jung RT, Sato T. Numerical simulation of high Schmidt number flow on unstructured hybrid mesh. Journal of Computational Physics. 2004;**203**:221-249

[9] Sloan ED. Clathrate hydrate of natural gases. New York: Dekker; 1998

[10] Aya I, Yamane K, Nariai H. Solubility of CO_2 and density of CO_2 hydrate at 30MPa. Energy. 1997;**22**:263-271

[11] Yang SO, Yang IM, Kim YS, Lee CS. Measurement and prediction of phase equilibria for water + CO_2 in hydrate forming condition. Fluid Phase Equilibria. 2000;**175**:75-89

[12] Servio P, Englezos P. Effect of temperature and pressure on the solubility of carbon dioxide in water in the presence of gas hydrate. Fluid Phase Equilibria. 2001;**190**:127-134

[13] Clarke MA, Bishnoi PR. Determination of the intrinsic rate constant and activation energy of CO_2 gas hydrate decomposition using in-situ particle size analysis. Chemical Engineering Science. 2004;**59**:2983-2993

[14] Sean W, Sato T, Yamasaki A, Kiyono F. CFD and experimental study on methane hydrate dissociation part II. General cases. AICHE Journal. 2007;**53**:2148-2160

[15] Nihous GC, Masutani SM. Notes on the dissolution rate of gas hydrates in undersaturated water. Chemical Engineering Science. 2006;**61**:7827-7830

[16] O'Connor RM, Fredrich JT. Microscale flow modelling in geologic materials. Physics and Chemistry of the Earth, Part A: Solid Earth and Geodesy. 1999;**24**(7):611-616

[17] Piller M, Nolich M, Favretto S, Radaelli F, Rossi E. Analysis of hydraulic permeability in porous media: From high resolution X-ray tomography to direct numerical simulation. Transport in Porous Media. 2009;**80**(1):57-78

[18] Sahimi M. Flow and Transport in Porous Media and Fractured Rock. Weinheim: VCG; 1995

[19] Boomsma K, Poulikakos D, Ventikos Y. International Journal of Heat and Fluid Flow. 2003;**24**:825

[20] Fukumoto A, Sean WY, Sato T, Yamasaki A, Kiyono F. Estimation of dissociation rate constant of CO_2 hydrate in water flow. Greenhouse Gases: Science and Technology. 2015; **5**(2):169-179

[21] Pohlhausen E. Der Wärmeaustausch zwischen festen Körpern und Flüssigkeiten mit kleiner reibung und kleiner Wärmeleitung. Zeitschrift für Angewandte Mathematik und Mechanik. 1921;**1**:115-121. DOI: 10.1002/zamm.19210010205

[22] Shu SS, Lee MJ. Dynamic behavior of methane hydrates formation and decomposition with a visual high-pressure apparatus. Journal of the Taiwan Institute of Chemical Engineers. 2016;**62**:1-9

IntechOpen